

# MEASUREMENT-BASED DELAY PERFORMANCE ESTIMATION IN ATM NETWORKS

Seung Yeob Nam and Dan Keun Sung

Dept. of EECS, KAIST, 373-1, Kusong-dong, Yusong-gu, Taejeon, 305-701, KOREA, E-mail: synam@cnr.kaist.ac.kr, dksung@ee.kaist.ac.kr

*Abstract*—Real-time traffic requires strict delay constraints in terms of maximum cell transfer delay(CTD) and cell delay variation(CDV). In order to support the required quality of service (QoS) of each connection in ATM networks, it is important to estimate the current status of networks by using local information such as cell delay and delay variation in switches. We develop a framework for obtaining delay distribution in a single switch module by monitoring the internal buffer. We also propose a new delay estimation mechanism utilizing a fast convolution approximation scheme in order to reduce the number of operations and the required amount of the data for estimating end-to-end delay. The feasibility of the proposed delay estimation mechanism is verified by simulation for various types of CBR and VBR traffic loads.

## I. INTRODUCTION

Broadband Integrated Services Digital Networks (B-ISDN) are expected to meet various QoS requirements at the ATM layer. These QoS parameters include cell loss ratio(CLR), cell transfer delay(CTD), and cell delay variation(CDV). Demand for strict delay performance has grown as the amount of internet traffic explodes and new multimedia services such as VoIP emerge [1].

One important part of network management is to monitor the performance of networks. Network switches need to know the QoS level that they can support. During call setup, the network should estimate the end-to-end QoS level from source to destination using local information from local switches. It is important to accurately estimate end-to-end QoS for decreasing call blocking probability and for increasing network utilization.

Four methods have been proposed for estimating end-to-end CDV: a simple method [2], a square root method [3], an asymptotic method [4], and a Chernoff method [5]. The simple method [2] may overestimate the end-to-end CDV, which can increase call blocking probability and can decrease network utilization. The square root method [3] assumes that local CDV in a switch equals some constant times the standard deviation of CTD, where the constant is identical for all switches. However, the constant to be multiplied by the standard deviation may not be the same for all switches. The asymptotic method [4] yields good performance in terms of accuracy. But, the asymptotic method is complex and difficult to implement. The Chernoff method [5] assumes that queueing delay in a switch is gamma distributed. But recent studies have demonstrated that a compressed video source shows a long-range dependence(LRD) property [6]. Therefore, the assumption of gamma distribution may not hold in general.

In this paper we propose a new delay estimation method which yields good performance. The proposed method is based on the fast convolution approximation [7]. For a multistage switch or multiple nodes it is possible to obtain end-to-end delay characteristics through consecutive convolutions if correlation between the delays of successive nodes is negligible. But due to constraints on signaling parameters [8], conventional convolution mechanisms are not feasible. We use the fast convolution approximation method to overcome this problem.

Derivation of local delay distribution is also an important problem. One conventional approach is to directly measure delay in ATM networks by using time stamps in OAM or test cells [9][10]. However, if time stamps are used for only OAM cells, it is very complicated to analyze the delay characteristics for various connections between input and output ports.

Another approach is queueing analysis based on input traffic modeling. Input traffic models include Bernoulli process, interrupted Bernoulli process [11], Markov modulated Poisson process(MMPP) [12] [13]. In real situations various traffic types such as voice and video can pass a switch through the same output port of an output buffered switch. This dynamic traffic characteristic makes real-time queueing analysis infeasible. Therefore, measurement of traffic or queueing behavior is inevitable. In this paper we propose a delay estimation method which monitors the buffers of an output buffer type ATM switch. The proposed method can estimate the cell delay distribution for various input traffic, and it can also be applied to shared buffer type ATM switches.

This paper is organized as follows. In Section II, we derive delay distributions from the information obtained by monitoring the buffers of output-buffered ATM switch. In Section 3, we consider how to obtain the delay performance for a multistage switch. In Section 4, we verify the derived relations by simulation. Finally, we conclude in Section 5.

## II. PREDICTION OF CELL DELAY DISTRIBUTION THROUGH MONITORING BUFFERS

CTD is composed of several components. These components include transmission delay, fixed switching delay and queueing delay. While transmission delay and switching delay are fixed for a given connection, queueing delay varies depending on the loading of the given network. In this paper we focus on the queueing delay component.

### A. Single ATM Switch Module

In this paper, we consider an ATM switch which is an  $m \times m$  output-buffered switch shown in Fig. 1. Cells arrive simultaneously at any inlets destined to a single output.

---

<sup>1</sup>This work was supported in part by the Basic Research Program of the Korea Science and Engineering Foundation.

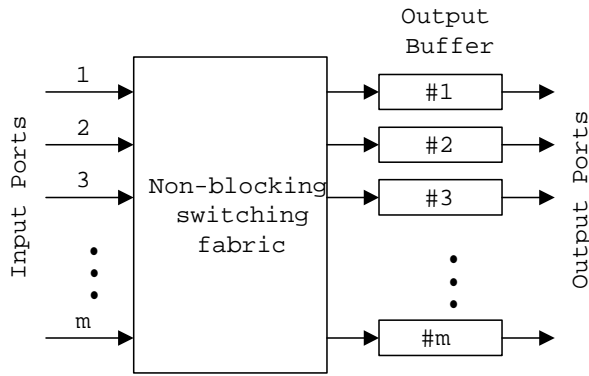


Fig. 1. An  $m \times m$  single ATM switch module

To ensure that no cells are lost in the switching fabric, cell transfer should be performed at  $m$  times the speed of inlets. The system should be able to write  $m$  cells in the output queues during one input cell time. The control of output queues is based on a simple FIFO discipline to ensure that cells remain in the correct sequence.

### B. Relation between buffer length distribution and cell delay distribution

We model an output buffer as a single queue system, as shown in Fig. 2. Traffic streams from  $m$  input ports ( $l_1, l_2, \dots, l_m$ ) enter the queue. Cells arrive in the discrete time slot, and service time is deterministic. Output link utilization is defined as the ratio of the number of busy slots to the number of total time slots. Let  $N$  be the buffer size observed at a random time slot. Then, we can obtain the following relation between the output link utilization  $U_{out}$  and the probability that the buffer is empty at random times.

$$U_{out} = 1 - Pr(N = 0) \quad (1)$$

When the buffer capacity is  $K$ , if we let  $W$  and  $N^-$  denote the waiting time of a cell in the queue and the system size observed by an arriving cell, respectively, the following relations hold.

$$Pr(W = i) = \frac{Pr(N^- = i)}{1 - Pr(N^- = K)}, \quad i = 0, 1, \dots, K-1. \quad (2)$$

$$Pr(N = n) = U_{out} \frac{Pr(N^- = n-1)}{1 - Pr(N^- = K)}, \quad n = 1, 2, \dots, K. \quad (3)$$

Combining (1), (2), and (3) yields the following equation:

$$Pr(W = i) = \frac{Pr(N^- = i)}{1 - Pr(N^- = K)} = \frac{Pr(N = i+1)}{1 - Pr(N = 0)}, \quad i = 0, 1, \dots, K-1. \quad (4)$$

Equation (4) shows a relationship among the distribution of the buffer size observed by an arriving cell, that of buffer size observed at random times, and that of cell waiting time.

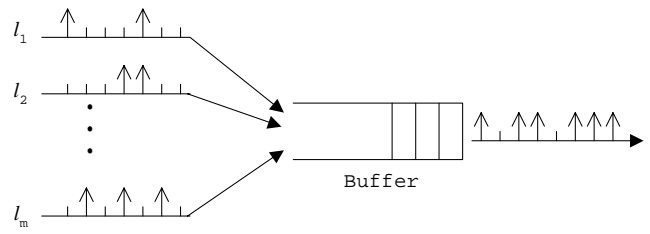


Fig. 2. A single queue system

Thus, it is possible to obtain the delay distribution by monitoring the buffer at the instant of each cell arrival or by monitoring it every cell time by using (4).

We consider the relation between buffer size and cell delay distribution for an output-buffered ATM switch. Furthermore, if cells are managed separately according to their destined output port for a shared buffer ATM switch, we can consider a set of cells that are destined for the same output port as one queue. Therefore, the results of this section can also be applied to shared-buffer type ATM switches without modification.

### III. CELL DELAY PERFORMANCE FOR A MULTISTAGE SWITCH/MULTIPLE NODE

Thus far, we have considered cell delay performance at a single switch module. We now extend the analysis to multistage switches or multiple nodes.

If correlation of delays experienced in consecutive multiplexing nodes is negligible, convolution of the delay distribution of each multiplexing node becomes a good approximation for the distribution of the end-to-end delay [14]. However, if a small positive correlation exists, the convolution slightly underestimates the variance of the end-to-end delay of that connection. An experiment indicated that delays introduced in consecutive multiplexing nodes are almost uncorrelated [14]. Delay information at each node should be transferred to adjacent nodes in order to obtain the end-to-end delay distribution for a multistage switch by convolution. However, due to signaling constraints, it is impractical to transmit all probability values of the probability mass function (PMF) of the local delay. In this section we consider the application of our proposed fast convolution approximation scheme [7] to reduce the calculation time and the amount of transmitted data. Our algorithm uses the following property:

**Property 1.** Let  $X_1$  and  $X_2$  be discrete random variables that take integer values and satisfy the following condition for an integer  $k$ :

$$Pr(X_1 \geq k) = \sum_{i=k}^{\infty} Pr(X_1 = i) \leq \sum_{i=k}^{\infty} Pr(X_2 = i) = Pr(X_2 \geq k) \quad (5)$$

Letting  $Z_1 = X_1 + Y$ ,  $Z_2 = X_2 + Y$ , for a nonnegative discrete random variable  $Y$  independent of both  $X_1$  and  $X_2$ ,

the following relation holds:

$$Pr(Z_1 \geq k') \leq Pr(Z_2 \geq k'), \quad \forall k'$$

This indicates that the delay distribution of poor performance yields poor delay characteristics after convolution with an independent delay distribution. If a delay distribution is given, the values of the CDV, the maximum CTD, and the  $(1-\alpha)$  quantile CTD can be estimated [2]. The CDV can be calculated as a subtraction of the minimum delay from the  $(1-\alpha)$  quantile CTD in the delay distribution. It is possible to obtain the lower bound of minimum delay by summing the fixed delay of each node. Hence, the major role of delay distribution is to provide values for the  $(1-\alpha)$  quantile CTD or the maximum CTD. We introduce a fast algorithm that provides an upper bound for the  $(1-\alpha)$  quantile CTD with a small amount of data.

For a random variable  $X_1$  with a PMF of:

$$P_{X_1}(i) = Pr(X_1 = i) = \begin{cases} a_i, & \text{if } i \geq 0, \\ 0, & \text{otherwise,} \end{cases}$$

if we introduce  $X_2$  with the following PMF using data compression factor  $\Delta$ , which is a positive integer:

$$P_{X_2}(i) = Pr(X_2 = i) = \begin{cases} \sum_{h=i-\Delta+1}^i a_h, & \text{if } i=j\Delta-1, j=1, 2, \dots, \\ 0, & \text{otherwise,} \end{cases} \quad (6)$$

then the following relation holds for a nonnegative integer  $k$ :

$$Pr(X_1 \geq k) = \sum_{i=k}^{\infty} a_i \leq \sum_{i=\lceil k/\Delta \rceil \Delta}^{\infty} a_i = Pr(X_2 \geq k) \quad (7)$$

$X_1$  and  $X_2$  satisfy the condition of the Property 1. Thus, convolution of the PMFs of  $X_2$  and a discrete random variable  $Y_1$  yields the upper bound of the complementary cumulative distribution function (CDF) that can be obtained from convolution of the PMFs of  $X_1$  and  $Y_1$ . Since the random variable  $X_2$  retains compressed information about  $X_1$ , it is possible to reduce the amount of required data by use of  $X_2$  instead of  $X_1$ .

Information about random variable  $Y_1$  can also be compressed into  $Y_2$  by the same mechanism, as follows:

$$P_{Y_2}(i) = \begin{cases} \sum_{h=i-\Delta'+1}^i P_{Y_1}(h), & \text{if } i=j\Delta'-1, j=1, 2, \dots, \\ 0, & \text{otherwise,} \end{cases} \quad (8)$$

where  $\Delta'$  is a positive integer.

The convolution of PMFs of  $X_2$  and  $Y_2$  can be calculated as follows when  $\Delta$  is equal to  $\Delta'$ :

$$P_{X_2} * P_{Y_2}(k) = \begin{cases} \sum_{i=0}^k P_{X_2}(i) P_{Y_2}(k-i), & \text{if } k=n\Delta-2, n=2, 3, \dots, \\ 0, & \text{otherwise,} \end{cases} \quad (9)$$

$$\begin{aligned} P_{X_2} * P_{Y_2}(n\Delta-2) &= \sum_{i=0}^{n\Delta-2} P_{X_2}(i) P_{Y_2}(n\Delta-2-i) \\ &= \sum_{i=1}^{n-1} P_{X_2}(i\Delta-1) P_{Y_2}((n-i)\Delta-1) \\ &= \sum_{j=0}^{n-2} P_{X_2^*}(j) P_{Y_2^*}(n-2-j) \\ &= P_{X_2^*} * P_{Y_2^*}(n-2), \end{aligned} \quad (10)$$

where  $P_{X_2^*}(i) = P_{X_2}((i+1)\Delta-1)$  and  $P_{Y_2^*}(i) = P_{Y_2}((i+1)\Delta-1)$  for  $i=0, 1, 2, \dots$ .

This result indicates that convolution of the PMFs of  $X_2$  and  $Y_2$  can be obtained by convolution of  $P_{X_2^*}(i)$  and  $P_{Y_2^*}(i)$ , followed by rescaling. Let the maximum values of  $X_1$  and  $Y_1$  be  $D_X$  and  $D_Y$ , respectively. The number of probability values of  $P_{X_2^*}(i)$  is approximately  $1/\Delta$  times less than for  $P_{X_1}(i)$ . Therefore, convolution of the PMFs of  $X_2$  and  $Y_2$  instead of for  $X_1$  and  $Y_1$  can reduce the number of multiplications from  $(D_X+1) \times (D_Y+1)$  to  $(\lfloor D_X/\Delta \rfloor + 1) \times (\lfloor D_Y/\Delta \rfloor + 1)$ .

When  $\Delta$  is different from  $\Delta'$ ,  $\Delta^*$  denotes the greatest common divisor (GCD) of  $\Delta$  and  $\Delta'$ . Then, the number of multiplications can be reduced from  $(D_X+1) \times (D_Y+1)$  to  $(\lfloor D_X/\Delta^* \rfloor + 1) \times (\lfloor D_Y/\Delta^* \rfloor + 1)$  by the proposed mechanism. Increasing  $\Delta^*$  can reduce the number of operations at any level at the expense of approximation errors. If the GCD of  $\Delta$  and  $\Delta'$  is 1, the amount of data to transmit can be reduced but the convolution operation time is not reduced. In order to improve this condition we confine  $\Delta$  to a power of 2.

We consider how to calculate the  $(1-\alpha)$  quantile CTD for a 3-stage switch using the convolution approximation method. Fig. 3 shows how to determine  $\Delta$  for  $n_{th} = 3$  where  $n_{th}$  is the threshold value that limits the required amount of data. At each node a  $(1-\sqrt[3]{\alpha})$  quantile CTD value  $d_\alpha$  is calculated. The minimum  $n$  which satisfies  $2^n \geq d_\alpha$  is given by:

$$n^* = \lceil \log_2 d_\alpha \rceil. \quad (11)$$

If we determine  $\Delta$  by

$$\Delta = \begin{cases} 1, & \text{if } n^* \leq n_{th}, \\ 2^{n^* - n_{th}}, & \text{if } n^* > n_{th}, \end{cases} \quad (12)$$

the interval  $[0, 2^{n^*}]$  is divided into less than  $2^{n_{th}}$  subsections of length  $\Delta$ . The reason to determine  $\Delta$  based on the  $(1-\sqrt[3]{\alpha})$  quantile CTD is that it may require a large amount of samples to obtain the  $(1-\alpha)$  quantile CTD when  $\alpha$  is very small.

The end-to-end  $(1-\alpha)$  quantile CTD can be obtained by successive convolutions if there are probability values less than or equal to  $\sqrt[3]{\alpha}$  in the delay distribution of each node. Using  $\Delta$  determined by (11) and (12), if we generate a new PMF  $X_2$  by the mechanism of (6),  $P_{X_2^*}(i)$  is not larger than  $\sqrt[3]{\alpha}$  for all  $i$  larger than  $2^{n_{th}}$ . If we make new PMFs by the same mechanism at other nodes, the last probability value

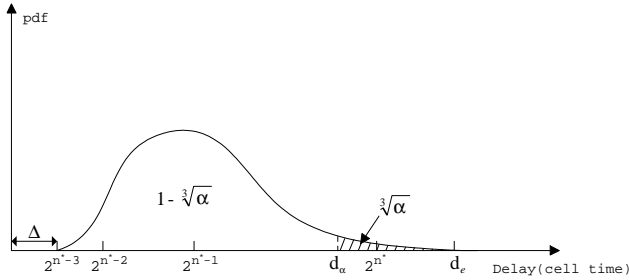


Fig. 3. Determination of  $\Delta$  for the fast convolution approximation when  $n_{th} = 3$

of each PMF is not larger than  $\sqrt[3]{\alpha}$ . Thus, consecutive convolutions yield a probability value smaller than  $\alpha$ , and the upper bound of the  $(1-\alpha)$  quantile CTD can be calculated.

Since both UNI and NNI signaling supports only one parameter for end-to-end CDV calculation, only one value can be passed from switch to switch [8]. If we assume  $d_e \leq 2d_\alpha$  in Fig. 3 where  $d_e$  is the maximum CTD, the number of probability values that need to be transferred between switches is at most four when  $n_{th}$  is 1. The asymptotic method requires 3 parameters to be signaled, and the Chernoff method requires 2 parameters to be signaled [5]. Thus, the number of parameters to be signaled is not excessively large compared with other methods.

## IV. SIMULATION RESULTS

### A. Input Traffic Model

We use four types of CBR source described in Table 1 and three types of VBR source described in Table 2 [15]. When multiple connections of the same traffic pattern are generated, the phase of each connection is randomized over the interarrival time of that traffic. VBR test sources are characterized as follows:

- A two-state Markov process consists of an active state and a silent state.
- The duration of an active phase has an integer number of cell times with a geometric distribution with a mean of  $M_a$ . The silent state lasts for an integer number of cell times, which is geometrically distributed with a mean of  $M_s$ .
- During the active state, a VBR test source emits a synchronous burst of cells, with a period of  $T$ , where  $T$  is an integer number of cell slots. The first cell of the burst occurs at the beginning of the active state. Thus, the mean burst size is given by  $B = M_a/T$  cells.

### B. Relation between the Distribution of Buffer Size and the Distribution of Cell Delay

We evaluate the performance of a switch shown in Fig. 1. The number of input ports and the number of output ports are both 32. Delay is measured between input and output ports. Input ports are based on Synchronous Optical Network (SONET) STS-3c.

We consider two methods to obtain the distribution of buffer lengths. The first method is to monitor the queue whenever a cell arrives and the second is to monitor the buffer every cell time to obtain the queue size distribution at an arbitrary time. We can estimate the cell delay distri-

TABLE 1  
CHARACTERISTICS OF CBR TEST SOURCES

CBR Source Type	CBR I	CBR II	CBR III	CBR IV
PCR(cells/sec.)	4,140	16,560	119,910	173
Load	0.0117	0.04688	0.33333	0.00049

TABLE 2  
CHARACTERISTICS OF VBR TEST SOURCES

VBR Source Type	VBR I	VBR II	VBR III
$M_a$ (cell slots)	240	500	210
$T$ (cell slots)	6	25	1
$M_s$ (cell slots)	720	2500	2500
Load	0.04167	0.00667	0.07749

butions from the queue length distribution observed by arriving cells and from the system size distribution at random times by using (4). On the other hand, the cell delay distribution can be measured through the time stamp of each cell. Fig. 4 compares the estimated cell delay distributions with the measured cell delay distribution when the traffic load is 0.454544. Two estimated graphs almost agree with the measured graph.

### C. Application of the fast convolution approximation to end-to-end delay estimation

We consider an end-to-end delay distribution for a three-stage switch and evaluate the fast convolution method by simulation. Fig. 5 illustrates a serially connected three buffer model. The CBR I traffic shown in Table 1 and the VBR I traffic shown in Table 2 are used as foreground traffic. All the traffic sources in Table 1 and 2 constitute background traffic.

Fig. 6 compares the distributions obtained by three different methods. The first method is to obtain the delay distribution by measuring the delay of each cell using a time stamp. The second method is to take convolutions after obtaining the delay distribution of each node. The third method is to use the fast convolution approximation explained in Section III. When the buffer capacity is  $K$ , the maximum number of probability values required to transmit for a convolution operation is  $K$ . However, if we use the fast convolution approximation method, the maximum amount of data does not exceed  $2^{n_{th}+1}$ . Thus, we can control the amount of data required for transmission using  $n_{th}$ . The larger the value of  $n_{th}$  becomes, the closer the upper bound of 1-CDF approaches the measured distribution, as shown in Fig. 6. However, the amount of data required for transmission increases. Note that the graph obtained by the conventional convolution agrees well with the graph obtained by time stamps.

Fig. 7 compares  $(1-\alpha)$  quantile CTDs obtained by three different methods according to  $\alpha$ . The foreground traffic is the VBR I source shown in Table 2, and  $n_{th}$  is 3 for the fast convolution. Although  $n_{th}$  is not large, the fast convolution yields a tight upper bound for the measured delay.

## V. CONCLUSIONS

We have obtained a relation among the queue size distribution observed by arriving cells, the queue size distribution at an arbitrary time, and cell delay distribution obtained by using the time stamp of each cell. Using this relation we can estimate the cell delay distribution in a single switch module by monitoring the buffer without using the time stamp of each cell for any type of input traffic. We showed the validity of this relation by simulation.

For a multistage ATM switch or multiple nodes we can estimate the end-to-end delay characteristics by successive convolutions of the delay distribution of each stage. We apply a fast convolution approximation mechanism in order to reduce the number of multiplications and the amount of data required for transmission. The fast convolution approximation yields a tight upper bound of the 1-CDF for the end-to-end delay. Thus, we can obtain a good estimation of the  $(1-\alpha)$  quantile CTD from this mechanism with fewer operations, compared with the conventional convolution. We evaluated the performance of the proposed delay estimation mechanism by simulation.

## REFERENCES

- [1] Elizabeth McPhillips, *The Factors Affecting the Growth of VoIP*, Hewlett Packard, 1999.
- [2] ATM Forum, *Traffic Management Specification*, Version 4.0, 95-0013R10, 1996.
- [3] ATM Forum, *B-ISDN Inter-Carrier Interface(BICI) Specification Version 1.1*, Sept. 1994.
- [4] M. Borden, "Properties of CDV and Its Accumulation," ATM Forum Contribution, Aug. 1995.
- [5] I. Korpeoglu, S. K. Tripathi, and X. Chen, "Estimating End-to-End Cell Delay Variation in ATM Networks," In *Proc. ICCT'98*, vol. 1, pp. 472-483, Oct. 1998.
- [6] J. Beran, R. Sherman, M. S. Taqqu, and W. Willinger, "Long-range dependence in variable bit rate video traffic," *IEEE Trans. Commun.*, vol. 43, no. 2/3/4, pp. 1566-1579, 1995.
- [7] Seung Y. Nam and Dan K. Sung, "Fast convolution approximation scheme for estimating end-to-end delay performance," *Electronics Letters*, vol. 36, no. 16, pp. 1432-1434, Aug. 2000.
- [8] ATM Forum, *User Network Interface Version 4.0*, 1996.
- [9] ITU-T Recommendation I.356, "B-ISDN ATM Layer Cell Transfer Performance," Oct. 1996.
- [10] C. Roppel, "Estimating Cell Transfer Delay in ATM Networks Using In-Service Monitoring Methods," In *Proc. IEEE GLOBECOM'95*, pp. 904-908, 1995.
- [11] J. M. Hah and M. C. Yuang, "Estimation-based call admission control with delay and loss guarantees in ATM networks," *IEE Proc. Commun.*, vol. 144, no. 2, Apr. 1997.
- [12] H. Heffes and D. M. Lucantoni, "A Markov modulated characterization of packetized voice and data traffic and related statistical performance," *IEEE J. Select. Areas Commun.*, vol. 4, pp. 856-868, 1986.
- [13] S. H. Kang, C. Oh, and D. K. Sung, "A Traffic Measurement-Based Modeling of Superposed ATM Cell Streams," *IEICE Trans. On Commun.*, vol. E80-B, no. 3, pp. 434-441, Mar. 1997.
- [14] D. Vleeschauer, "Experimental Verification of the Statistical Independence of Cell Delays Introduced in Consecutive Switches," In *B-ISDN Teletraffic Modelling Symposium*, pp. 105-116, Feb. 1995.
- [15] Bellcore, *Broadband Switching System (BSS) Generic Requirements*, GR-1110-CORE, Issue 1, Sep. 1994, Revision 3, Apr. 1996.

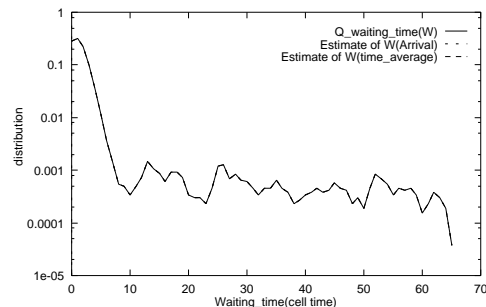


Fig. 4. Comparison of estimated and measured delay distributions when the input rate is equal to the output rate

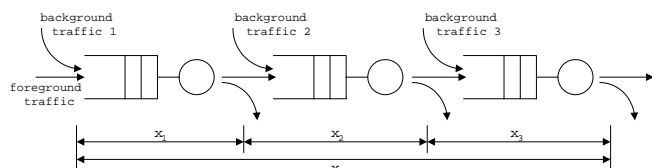


Fig. 5. Serially connected three buffer model

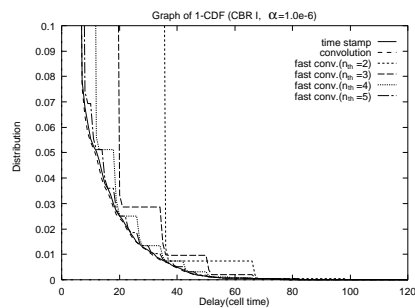


Fig. 6. Comparison of time stamp, convolution, and fast convolution approximation methods

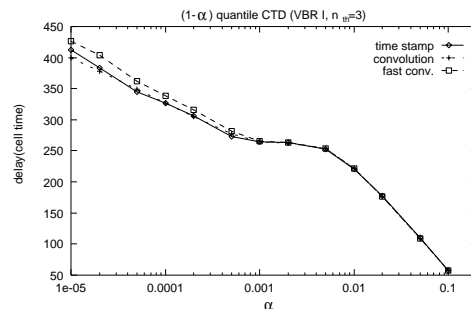


Fig. 7. Comparison of cell transfer delays obtained by various methods